Chapter 3

Dark Matter and Baryon Asymmetry of the Universe in a A_4 Modular Symmetric Model in ISS(2,3)

In this chapter we present our study on baryon asymmetry of the universe and dark matter by adding a scalar triplet $\eta = (\eta_1, \eta_2, \eta_3)$ to the particle content of minimal Inverse seesaw. We have realised this extension of minimal inverse seesaw with the help of a level 3 modular group, $\Gamma(3)$. This group is isomorphic to non-abelian discrete symmetry group A_4. After symmetry breaking, the neutral components of η i.e. η_2, η_3 are considered as dark matter candidates for this work. The heavy fermions in ISS(2,3) form two quasi-Dirac pairs. The decay of the lightest pair paves the way for baryon asymmetry. In order to check the consistency of our model with various experimental constraints, we have calculated the relic density of dark matter and tried to evaluate BAU through resonant leptogenesis. The model is able to produce a large value of these quantities in the desired range as required by different cosmological observations and also successfully produces neutrino masses and mixings in the allowed 3σ range. These results, along with their discussions are shown in later sections of the chapter.

3.1 Introduction

The shortcomings of Standard Model paved the way for development of many BSM mechanisms. These mechanisms have their own advantages and are successful in providing an appropriate roadmap to understand many of the BSM phenomena. One of the popular among the many different BSM formulations is Inverse seesaw. The additional particles in this mechanism includes three right-handed neutrinos and three sterile fermions, which are singlet fields under the SM gauge group. A minimal version of inverse seesaw contains only two right-handed neutrinos. This version which acts as the building block of our work is called Minimal Inverse seesaw, ISS(2,3). Moreover this mechanism enhances the possibility of detecting right-handed neutrinos by lowering their energy scale to TeV.

It is now an established fact that there is an asymmetry between matter and anti-matter in the universe. Cosmological observations indicate that the number of baryons in the universe is not equal to the number of anti-baryons. This difference in number between baryons and anti-baryons is termed as Baryon Asymmetry of the Universe (BAU) [160, 161, 86]. At the beginning, as evident from various considerations, the universe started with an equal number of both the types of particles i.e. baryons and anti-baryons. As such the asymmetry observed in the universe occured in much later times and must have been generated through a dynamical process called baryogenesis. As per Planck data, the value of this asymmetry, denoted by η_B is found to be [162]

$$\eta_B = (6.04 \pm 0.08) \times 10^{-10} \tag{3.1}$$

As proposed by Sakharov, three important conditions are necessary for baryogenesis: Baryon number violation (B), C and CP violation , interactions out of thermal equilibrium [163]. In the last couple of decades several attempts have been made to address the phenomena of BAU. One of the popular and successful theoretical process is baryogenesis via leptogenesis. This mechanism was first proposed by Fukugita and Yanagida [60]. According to this mechanism, the L-violating out of equilibrium decays of singlet neutrino creates an asymmetry in the leptonic sector. This excess in lepton number can be converted into the observed baryon asymmetry through B+L violating sphaleron processes [164, 165]. In this

regard, Inverse seesaw contains gauge singlet right-handed neutrinos and sterile fermions. As a result, the asymmetry generated by decay of one of the quasi-Dirac pairs formed by these particles can be converted into baryon asymmetry of the universe.

The presence of dark matter (DM), an inevitable mystery of the universe, has been well-established through various observations in astrophysics and cosmology. Some of the strong convictions in this regard are galaxy cluster observations by Fritz Zwicky [91], galaxy rotation curves [166], recent observation of the Bullet clusters [167] and cosmological data from the Planck collaboration [168]. All of these remarks suggest the existence of an unknown, non-luminous, non-baryonic dark matter which constitutes about 26% of the energy density of the universe and is approximately five times more than luminous matter. Currently the amount of dark matter in the universe as found from the Planck data is [78]

$$\Omega h^2 = 0.1199 \pm 0.0027 \tag{3.2}$$

This is called the relic density of dark matter. The properties that a candidate must have to qualify as a viable dark matter candidate has been highlighted in [169, 170]. Unfortunately, the SM particles do not possess these required criterias and so none of them can be considered to be a viable dark matter candidate. Therefore, from the particle physics view point, one has to extend the SM particle content by incorporating new fields to find a suitable candidate that could produce the correct relic abundance.

The discussions included here are the works done in a model which has been constructed by augmenting ISS(2,3) with a Higgs-type scalar field $\eta = (\eta_1, \eta_2, \eta_3)$, which is considered as triplet under A_4. Similar to the model discussed in first chapter, we have used a flavon field ϕ whose role is to make the charged lepton mass matrix diagonal. As mentioned earlier, the neutral components of η, after symmetry breaking, serves as the dark matter candidates for this work. In order to formulate the interactions among different fields, we have used A_4 modular symmetry and Z_3 discrete group. The development of this model has been discussed in detail in later sections of the chapter.

We have organised this chapter in the following manner: in section (3.2) we have

presented a detailed discussion about the model. Section (3.3) contains the process of leptogenesis in minimal inverse seesaw. Here we have discussed the methods that we have used to study and evaluate BAU in this work. In section (3.4) we provide the roadmap that we have adopted to calculate the relic density of dark matter. The analysis and discussion of the results of the work have been presented in section (3.5). Finally in section (3.6) we conclude this chapter by providing a brief summary of the work.

3.2 Description of the Model

Here in this section we will discuss in detail about the model related to the work of this chapter. In this case, we have extended the particle content of ISS(2,3) by adding an extra particle to it. This new addition is a Higgs-type triplet scalar field $\eta = (\eta_1, \eta_2, \eta_3)$. The motivation behind the inclusion of this scalar field lies in the possibility of its neutral components being a probable dark matter candidate for our work. The level $N = 3$ modular group $\Gamma(3)$ which is isomorphic to A_4, plays a crucial role in development of the model. Because of this reason we have extensively used the discrete symmetry A_4 group in the model. Along with this symmetry group, Z_3 also facilitates to get the desired terms of the Lagrangian of the work.

In comparison to the conventional inverse seesaw, there are two right-handed neutrinos (N_1, N_2) and three singlet sterile fermions (S_1, S_2, S_3) in the minimal inverse seesaw mechanism. Due to this reason the order of M_D, M_{NS} changes to 3×2 and 2×3; whereas for M_S it remains unchanged. The VEV alignment of the flavon ϕ facilitates to get a diagonal charged lepton mass matrix. As such the role of this flavon is restricted only to the charged lepton sector without affecting the neutrino sector. The three weight 2 modular forms (Y_1, Y_2, Y_3) of $\Gamma(3)$ are considered as triplets under A_4 symmetry. The right-handed neutrinos (N_1 and N_2) in the model are taken as singlets under A_4 and they transform as $1'$ and $1''$, respectively; while the sterile neutrinos (S_i) and lepton doublets (L) are considered as triplets. The modular weight of the right-handed neutrinos is taken as -3, the lepton doublets (L) is +1 where as for sterile neutrinos and η it is taken

to be zero. We have introduced two weighton fields, β_1 and β_2, in this model. These are Standard Model singlet fields with non-zero modular weights and are associated with the mass terms of right-handed neutrinos [127]. In our work we have taken the weightons to be singlet under A_4 and their modular weight is +1. The above discussions about how the different fields transform under various groups in the model have been highlighted in Table (3.1).

Fields	L	N_1	N_2	S_i	H	ϕ	η
A_4	3	$1'$	$1''$	3	1	1	3
Z_3	ω^2	1	1	1	ω^2	ω	ω
K_I	1	-3	-3	0	-1	2	0

Table 3.1: Charge assignments of the particles under the various groups considered in the model. K_I refers to the modular weights.

As we have considered a DM candidate in our model, it is necessary to introduce a discrete symmetry Z_2 in order to maintain stability of the DM candidate. The SM particles remain Z_2 even whereas the right handed neutrino and the newly added field eta are odd under this symmetry. After electroweak symmetry breaking, one of the η's acquire VEV and their form can be written as [171, 172]:

$$\eta_1 = \begin{pmatrix} \eta_1^+ \\ \frac{v_\eta + h_1 + iA_1}{\sqrt{2}} \end{pmatrix}, \quad \eta_2 = \begin{pmatrix} \eta_2^+ \\ \frac{h_2 + iA_2}{\sqrt{2}} \end{pmatrix}, \quad \eta_3 = \begin{pmatrix} \eta_3^+ \\ \frac{h_3 + iA_3}{\sqrt{2}} \end{pmatrix} \tag{3.3}$$

As mentioned in [172], the VEV alignment of η can be written as $\eta = v_\eta(1,0,0)$ and η_2, η_3 will be the dark matter candidates. Moreover we get a diagonal charge lepton mass matrix when the VEV of ϕ is taken as $\phi = (u,0,0)$ [14]. So the Lagrangian for the charged leptons can be written as:

$$L_L = \alpha_1 E_1^c H_d (L\phi)_1 + \alpha_2 E_2^c H_d (L\phi)_{1'} + \alpha_3 E_3^c H_d (L\phi)_{1''} \tag{3.4}$$

In the above equation, the parameters $\alpha_1, \alpha_2, \alpha_3$ can be adjusted to get the desired masses of the charged leptons. Accordingly the mass matrix is found to be: $M_L = diag(\alpha_1, \alpha_2, \alpha_3)uv$. Here v is the vaccum expectation value of the Higgs field. Now based on the above discussions about relevant charge assignmets, the Yukawa Lagrangian for the neutrino sector can be written as:

$$\mathcal{L} = N_1(LY)_3\eta + N_2(LY)_3\eta + \beta_1 N_1(SY)_{1''} + \beta_2 N_2(SY)_{1'} + \mu_0(SS)_1 \tag{3.5}$$

The first two terms in the Lagrangian denotes the interaction between left-handed and right-handed neutrinos. The next two terms represents the interaction between N's and S's while the last term denotes the interaction between the sterile fermions. With the help of eq. (3.5), we can write down the corresponding neutrino mass matrices in the following way. The Dirac mass matrix of order 3×2 for the neutrinos can be written as:

$$M_D = v_\eta \begin{pmatrix} -Y_1 & -Y_2 \\ 2Y_2 & -Y_1 \\ -Y_1 & 2Y_3 \end{pmatrix} \tag{3.6}$$

v_η in eq. (3.6) is the VEV of η. Similarly, following the A_4 multiplication rules, the Majorana mass matrix for right-handed neutrino and sterile fermions, and the lepton number violating mass term for the sterile fermions can be written as:

$$M_{NS} = \begin{pmatrix} \beta_1 Y_3 & \beta_1 Y_2 & \beta_1 Y_1 \\ \beta_2 Y_2 & \beta_2 Y_1 & \beta_2 Y_3 \end{pmatrix}, \qquad M_S = \mu_0 \begin{pmatrix} 1 & 0 & 0 \\ 0 & 0 & 1 \\ 0 & 1 & 0 \end{pmatrix} \tag{3.7}$$

Following the methods as mentioned earlier, the full 8×8 neutrino mass matrix for ISS(2,3) can be written as:

$$\mathcal{M} = \begin{pmatrix} 0 & M_D^T & 0 \\ M_D & 0 & M_{NS} \\ 0 & M_{NS}^T & M_S \end{pmatrix}_{8\times8} \tag{3.8}$$

This 8×8 matrix $\mathcal{M}$ in eq (3.8) can be diagonalised with the help of an Unitary matrix, $\mathcal{U}$ as

$$\mathcal{U}^\mathcal{T} \mathcal{M} \mathcal{U} = M_{diag} = diag(m_1, m_2, m_3, ..., m_8) \tag{3.9}$$

where m_i's in the above equation are masses of the particles of the model. In order to obatin the mass matrix for the active neutrinos one can use the expression given by eq. (2.12). Diagonalising this 3×3 matrix will yield the eigenvalues for the three active neutrinos. Thus we have constructed this model using A_4 modular symmetry in the framework of ISS(2,3). The scalar field η is the new particle added to this model. Apart from producing the neutrino parameters in the allowed experimental ranges, we have also used this model to study BAU and dark matter.

3.3 Leptogenesis in ISS(2,3)

In order to validate our model considering the cosmological constraints, we try to generate the observed baryon asymmetry of the universe through leptogenesis. There are five heavy neutrinos in ISS(2,3). As already mentioned, two of them are right handed neutrinos (N_1, N_2) and the other three are gauge singlet neutral sterile fermions (S_i). Four of these heavy particles form two pairs, called quasi-Dirac pairs, and one of them gets decoupled. Interestingly, the mass splitting between these pairs is comparable to their decay width. Among them the out-of-equilibrium decay of the lightest pair to any lepton flavor creates an asymmetry in the leptonic sector. This asymmetry created by decay of the lightest heavy neutrinos can be converted into baryon asymmetry through sphaleron processes [148, 173, 174]. On the other hand, asymmetry generated by decay of the heavier pair is washed out by lepton number violating scatterings of the lightest pair, thereby, it does not contribute to the asymmetry produced.

3.3.1 Computation of CP asymmetry

To calculate the CP-asymmetry we need the mass matrix for the heavy neutrinos. This matrix can be written as:

$$M_H = \begin{pmatrix} 0 & M_{NS} \\ M_{NS}^T & M_S \end{pmatrix} \tag{3.10}$$

Now on diagonalising the above matrix, one can get masses of the five heavy neutrinos. Also the mass splitting between the degenerate pairs is proportional to M_S.

$$M_{diag} = V^T M_H V = diag(m_1, m_2, m_3, m_4, m_5) \tag{3.11}$$

To diagonalise this 5×5 matrix analytically is a challenging and formidable task. So we opt for numerical diagonalisation so as to simplify our analysis. Again for the calculation of CP-asymmetry, a particular basis is preferred in which the matrix M_H becomes diagonal. In this basis the Lagrangian takes the form:

$$\mathcal{L}_{\mathcal{S}} = h_{i\alpha} N_i \eta L_\alpha + M_i N_i^T C^{-1} N_i + h.c. \tag{3.12}$$

where $h_{i\alpha}$ corresponds to the couplings in diagonal mass basis and N_i are the mass eigenstates of the four non-decoupled heavy fermions. Their relation to the

couplings in the flavor basis are represented by the following expressions [175, 90]:

$$\begin{aligned} h_{1\alpha} &= V_{11}^{*}\, y_{1\alpha} + V_{12}^{*}\, y_{2\alpha} \\ h_{2\alpha} &= V_{21}^{*}\, y_{1\alpha} + V_{22}^{*}\, y_{2\alpha} \\ h_{3\alpha} &= V_{13}^{*}\, y_{1\alpha} + V_{23}^{*}\, y_{2\alpha} \\ h_{4\alpha} &= V_{14}^{*}\, y_{1\alpha} + V_{24}^{*}\, y_{2\alpha} \end{aligned} \tag{3.13}$$

For the decay $N_i \to l_\alpha \eta$ $(\bar{l_\alpha}\eta)$, the formula for calculating the CP asymmetry ϵ_i by summing over the SM flavor α is given by [176]

$$\epsilon_i = \frac{\sum_\alpha[\Gamma(\tilde{\psi} \to l_\alpha \eta) - \Gamma(\tilde{\psi} \to \bar{l_\alpha}\eta^\dagger)]}{\sum_\alpha[\Gamma(\tilde{\psi} \to l_\alpha \eta) + \Gamma(\tilde{\psi} \to \bar{l_\alpha}\eta^\dagger)]} = \frac{1}{8\pi}\sum_{i\neq j}\frac{Im[(hh^\dagger)_{ij}^2]}{(hh^\dagger)_{ii}} f_{ij} \tag{3.14}$$

For the case of resonant leptogenesis, f_{ij} is the self energy correction term. Its expression is $f_{ij} = \frac{(M_i^2 - M_j^2)M_i M_j}{(M_i^2 - M_j^2)^2 + (M_i\Gamma_i + M_j\Gamma_j)^2}$. M_i and M_j are the real and positive eigenvalues of the heavy neutrino mass matrix. Γ_i is the decay width of one of the quasi-Dirac pair which is expressed as $\Gamma_i = \frac{M_i}{8\pi}(hh)_{ii}^\dagger$. Thus the explicit form of CP parameter for the decay of a quasi-Dirac pair, say (N_1, S_1), can be expressed as:

$$\begin{aligned} \epsilon_1 &= \frac{1}{8\pi(hh^\dagger)_{11}}\mathrm{Im}[(hh^\dagger)_{12}^2 f_{12} + (hh^\dagger)_{13}^2 f_{13} + (hh^\dagger)_{14}^2 f_{14}] \\ \epsilon_2 &= \frac{1}{8\pi(hh^\dagger)_{22}}\mathrm{Im}[(hh^\dagger)_{21}^2 f_{21} + (hh^\dagger)_{23}^2 f_{23} + (hh^\dagger)_{24}^2 f_{24}] \end{aligned} \tag{3.15}$$

As already mentioned, the asymmetry produced by decay of the heavier pair is washed out. Thus the wash out parameter for such decays, in terms of the Hubble parameter H, is written as:

$$K_i = \frac{\Gamma_i}{H} = \frac{M_i}{8\pi}(hh)_{ii}^\dagger \times \frac{M_{pl}}{1.66\sqrt{g*}M_i^2} \tag{3.16}$$

In the above equation, M_{pl} is the Planck mass and $g*$ denotes the effective number of relativistic degrees of freedom. The final expression for BAU can be written as:

$$Y_B = 10^{-2}\sum \kappa_i \epsilon_i \tag{3.17}$$

where κ_i is the dilution factor responsible for washout out of the asymmetry associated with the heavy pair. ϵ_i is the CP asymmetry generated in the leptonic sector. The expressions for κ_i depends on the values of washout factor in eq

(3.16). These relations can be summarised as [177]:

$$\begin{aligned} -\kappa &\approx \sqrt{0.1K}\ \ exp[\frac{-4}{3(0.1K)^{0.25}}], \qquad \text{for} K \geq 10^6 \\ &\approx \frac{0.3}{K(\ln K)^{0.6}}, \qquad\qquad\qquad \text{for}\ \ 10 \leq K \leq 10^6 \\ &\approx \frac{1}{2\sqrt{K^2+9}}, \qquad\qquad\qquad \text{for}\ \ 0 \leq K \leq 10 \end{aligned} \tag{3.18}$$

Thus, we use eq (3.17) to calculate the value of BAU in the framework of ISS(2,3). In our work we have computed the values of this asymmetry for both the hierarchies. We have highlighted our findings in the results and discussion section of the chapter. We find that for both the hierarchies there are a large number of points that satisfy the Planck value of BAU.

3.4 Dark matter

At the beginning of the universe the particles present in the thermal pool were in thermal equilibrium with each other. This implies that the rate at which lighter particles combined to form heavy particles and vice-versa was the same. During the course of evolution, the conditions that were required to maintain this equilibrium state were disturbed. As a result, after a certain temperature the density of some particle species became too low. Once this is achieved, the abundance of those particle remains the same and their density becomes constant. This phase of the particle species is called freeze-out and the density hereafter is referred to as relic density. For a particle χ, which was in thermal equilibrium, the relic density can be obtained from the Boltzman equations [178, 179]:

$$\frac{dn_\chi}{dt} + 3\mathcal{H}n_\chi = -<\sigma v> \left(n_\chi^2 - \left(n_\chi^{eqb}\right)^2\right) \tag{3.19}$$

In the above equation n_χ is the number density of the dark matter particle whereas n_χ^{eqb} is the density of χ when it was in equilibrium with the thermal bath. Here $\mathcal{H}$ represents the Hubble constant and $<\sigma v>$ is the thermally averaged annihilation cross-section of the dark matter candidate. For the interactions in eq. (3.5), the cross-section formula can be writtern as [180]:

$$<\sigma v> = \frac{v^2 y^4 m_\chi^2}{48\pi(m_\chi^2 + m_\psi^2)^2} \tag{3.20}$$

where the parameters m_χ, m_ψ and y represent the mass of the relic particle, mass of the Majorana fermion and the interaction between the dark matter and fermions in the model. v in the above expression represents the relative velocity of the relic particles whose value at the time of freeze-out is taken to be $0.3c$. The solution of eq. (3.19) in terms of reduced Hubble constant (h), as found in [181], can be written as:

$$\Omega_\chi h^2 = \frac{3 \times 10^{-27} \text{cm}^3 \text{s}^{-1}}{<\sigma v>} \tag{3.21}$$

The above expression of $\Omega_\chi h^2$ gives the relic density of dark matter particle. It is found that the self annihilation between dark matter and next to lightest neutral component of η contributes to the annihilation cross-section. For low mass region i.e. $m_{DM}<M_W$, the cross-section for the self annihilation of either η_2 or η_3 into Standard Model particles via the Higgs boson can be written as [182]:

$$\sigma_{xx} = \frac{|Y_f|^2|\lambda_x|^2}{16\pi s} \frac{(s-4m_f^2)^{\frac{3}{2}}}{\sqrt{s-4m_x^2}((s-m_h^2)^2+m_h^2\Gamma_h^2)} \tag{3.22}$$

where x is the dark matter particle (η_2, η_3) and λ_x is the coupling of x with the SM Higgs boson h. In eq. (3.22) Y_f represents the Yukawa couplings of the fermions. Γ_h represents the decay width of the SM Higgs and m_h is equal to 125 GeV. And s in the expression represents the thermally averaged center of mass squared energy and is given by $s = 4m_x^2 + m_x^2 v^2$, m_x is mass of the relic. In our work the neutral component of the scalar triplet η is the dark matter candidate. Moreover for the low mass region, the mass of the DM particle should be less than the mass of W boson, M_W [183]. The results that we have found in this work and their corresponding analysis are shown in the next section.

3.5 Numerical Analysis and Results

In this section we present the methodology and results of this work. Accordingly we diagonalise the 3×3 light neutrino mass matrix (m_ν) of the model by using the unitary mixing matrix, U_{PMNS}, to get the mass eigenvalues (m_1, m_2, m_3) of the active neutrinos. These eigenvalues which can be expressed in terms of solar and atmospheric mass squared differences have different forms for the two mass

hierarchy of neutrinos. For normal hierarchy they can be written in the form of a matrix as $diag(0, \sqrt{m_1^2 + \Delta m^2_{solar}}, \sqrt{m_1^2 + \Delta m^2_{atm}})$, whereas in the inverted ordering it takes the form $diag(\sqrt{m_3^2 + \Delta m^2_{atm}}, \sqrt{\Delta m^2_{atm} + \Delta m^2_{solar}}, 0)$ [184]. For numerical calculations, we have used the 3σ values of the oscillation parameters which are given in Table (2.3). Additional constraints on the model come from the two mass squared differences and sum of neutrino masses. Moreover the expressions in eq. (2.20) are used to calculate the three neutrino mixing angles.

For this work we find the real and imaginary components of the complex modulus τ in the range: Re(τ)→[-0.9, 0.9] and Im(τ)→[0.2, 6]. These ranges of the two components lie within the fundamental domain of τ. With these values of τ we can compute the Yukawa modular forms for both normal and inverted ordering. For further calculations we have taken μ_0 in the range [10, 20] KeV and v_η is considered in between $(30 - 50)$ GeV. In a similar way, we have taken the values of β_1 and β_2 in the ranges $[10^5, 10^6]$ GeV and $[10^2, 10^3]$ GeV, respectively, so as to obtain the values of different quantities in the allowed ranges. In the following parts of this section we will show the different plots and then discuss the respective results of this work.

3.5.1 Relation between the components of τ and mixing angles

Here we have demonstrated the relation that exists between Re(τ), Im(τ) of the complex modulus τ and the neutrino mixing angles for both the orderings. We find some specific regions for the former two quantities which could accomodate most of the values of these angles. The figures in (3.1) highlights these important observations. Although the real component of τ remains same for all the cases, the region for Im(τ) changes with respect to the angle in consideration. From the top two figures, we find that the allowed values of the atmospheric mixing angle (θ_{23}) lie in between (0.2 to 1.2) of Im(τ) for normal ordering, whereas for inverted ordering this range is found to be (0.4 to 1.0). The two figures in the middle is for solar mixing angle (θ_{12}). Interestingly for both the orderings the range of Im(τ) which fits the allowed data is found to be almost similar i.e. (0.3 to 6). From the bottom two figures we can find that the reactor mixing angle (θ_{13}) is

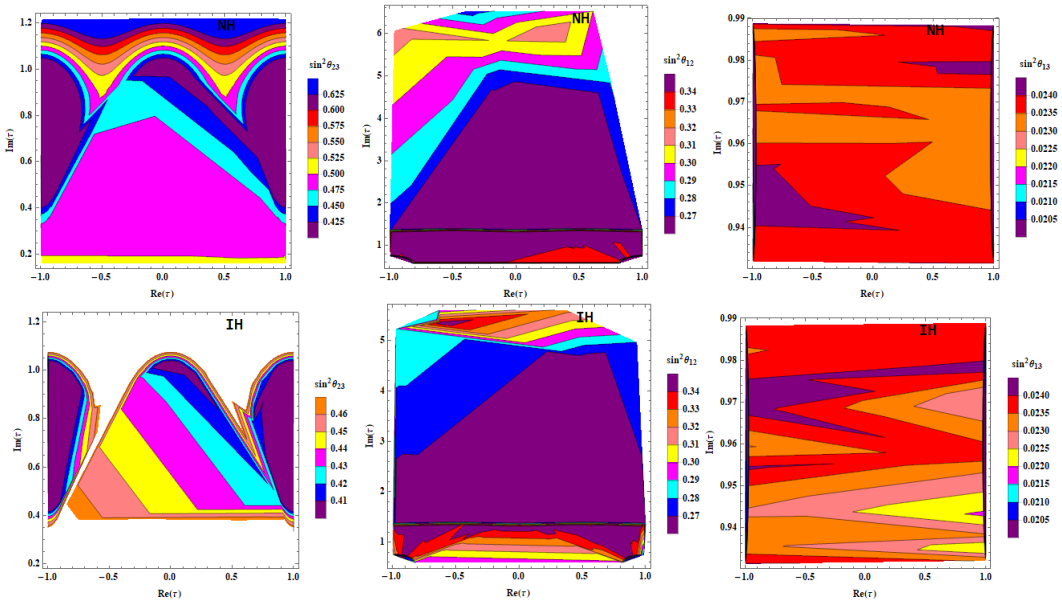

Figure 3.1: Corelation between real and imaginary parts of τ with the mixing angles for both the orderings.

confined to the region (0.8 to 1) of $\mathrm{Im}(\tau)$. Consequently we can find a common space of $\mathrm{Re}(\tau)$ and $\mathrm{Im}(\tau)$ for the three mixing angles: $-0.9 \leq \mathrm{Re}(\tau) \leq 0.9$ and $0.7 \leq \mathrm{Im}(\tau) \leq 1.0$.

3.5.2 Corelation between $\sin^2\theta_{12}$ and Yukawa modular forms

In the Fig. (3.2) we show the corelation between the Yukawa modular forms (Y_1, Y_2, Y_3) and solar mixing angle (θ_{12}). The two figures on the left are the contour plots for (Y_1, Y_2) with the mixing angle θ_{12}, the middle images are for (Y_1, Y_3) and the figures on the right are for (Y_2, Y_3). From these figures the ranges of the Yukawa modular forms can be found as: $0.9 \leq |Y_1| \leq 1.2$, $0.1 \leq |Y_2| \leq 2$, $0.1 \leq |Y_3| \leq 1.5$ for normal ordering and $0.9 \leq |Y_1| \leq 1.2$, $0.1 \leq |Y_2| \leq 1.8$, $0.1 \leq |Y_3| \leq 1.5$ for inverted ordering.

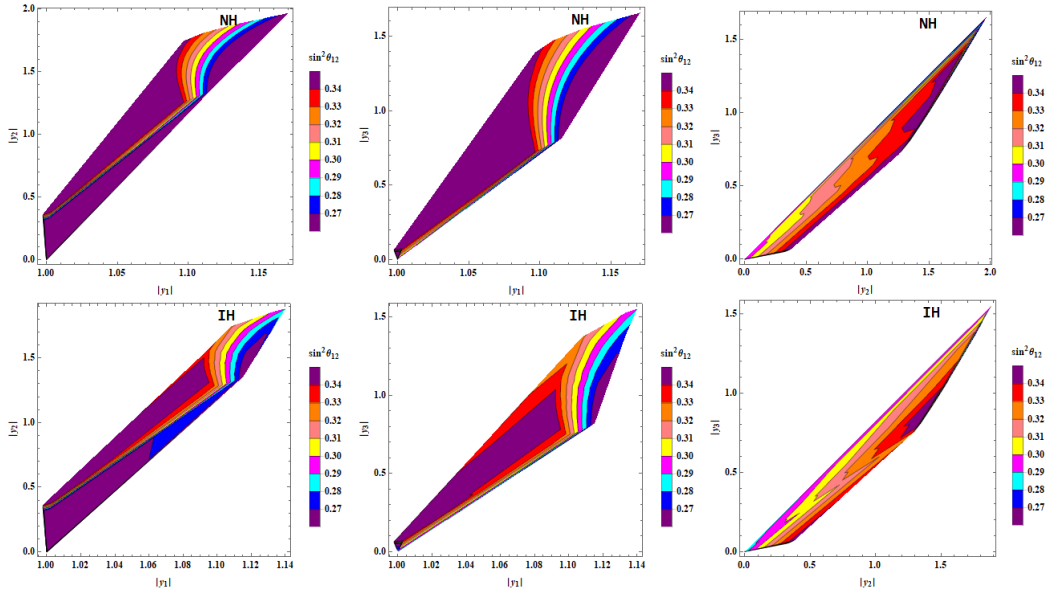

Figure 3.2: Contour plots of the Yukawa modular forms with the solar mixing angle (θ_{12}).

3.5.3 Corelation between $\sin^2\theta_{13}/\sin^2\theta_{23}$ and Yukawa modular forms

Similarly in Fig. (3.3) and (3.4) we show the contour plots of the Yukawa modular forms, reactor mixing angle (θ_{13}) and atmospheric mixing angle (θ_{23}). Accordingly we can find the ranges of Y_1, Y_2, Y_3 corresponding to the mixing angles from these figures. For the reactor mixing angle these ranges are: $1.024 \leq |Y_1| \leq 1.045$, $0.6 \leq |Y_2| \leq 0.9$, $0.2 \leq |Y_3| \leq 0.4$ for both normal and inverted ordering, whereas for the atmospheric mixing angle these ranges are found to be : $0.94 \leq |Y_1| \leq 1.02$, $0.5 \leq |Y_2| \leq 1.2$, $0.2 \leq |Y_3| \leq 0.9$ for normal ordering and $0.94 \leq |Y_1| \leq 1.02$, $0.5 \leq |Y_2| \leq 1.1$, $0.2 \leq |Y_3| \leq 0.7$ for inverted ordering. These values of the modular forms have been summarised in the Table (3.2). It is clear that the region of intersection for both the orderings lie around 0.9 to 1.2.

3.5.4 Contribution of η to BAU

In Fig. (3.5) we show the relation between the VEV of η and BAU. For normal ordering it can be seen that the Planck value of BAU does not have any correspondence to the mass of the scalar η. In other words, we can say that it does

	Normal Ordering	Inverted Ordering
$\|Y_1\|$	0.9-1.2	0.9-1.2
$\|Y_2\|$	0.5-1.8	0.1-1.8
$\|Y_3\|$	0.1-1.5	0.1-0.9

Table 3.2: This table shows the range of the modular forms corresponding to the mixing angles for both normal and inverted hierarchy.

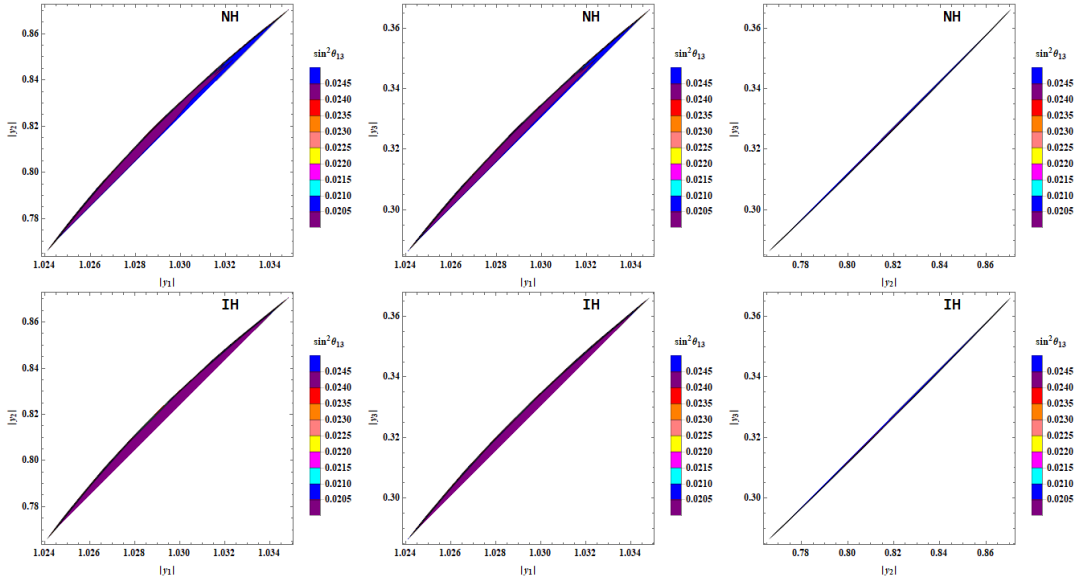

Figure 3.3: Contour plots of the Yukawa modular forms with the reactor mixing angle (θ_{13}).

not contribute to the study of leptogenesis. But for the case of inverted ordering, there are sufficient values of BAU within the Planck limit that corresponds to the mass of the scalar. This implies that for inverted ordering the scalar has some contribution to leptogenesis.

3.5.5 Corelation between BAU and lightest RHN M_1

In Fig. (3.6) we show the relation between BAU and lightest right-handed neutrino mass, M_1. We performed the calculations for both the hierarchies. From these graphs it is clear that for both the type of hierarchies there are sufficient

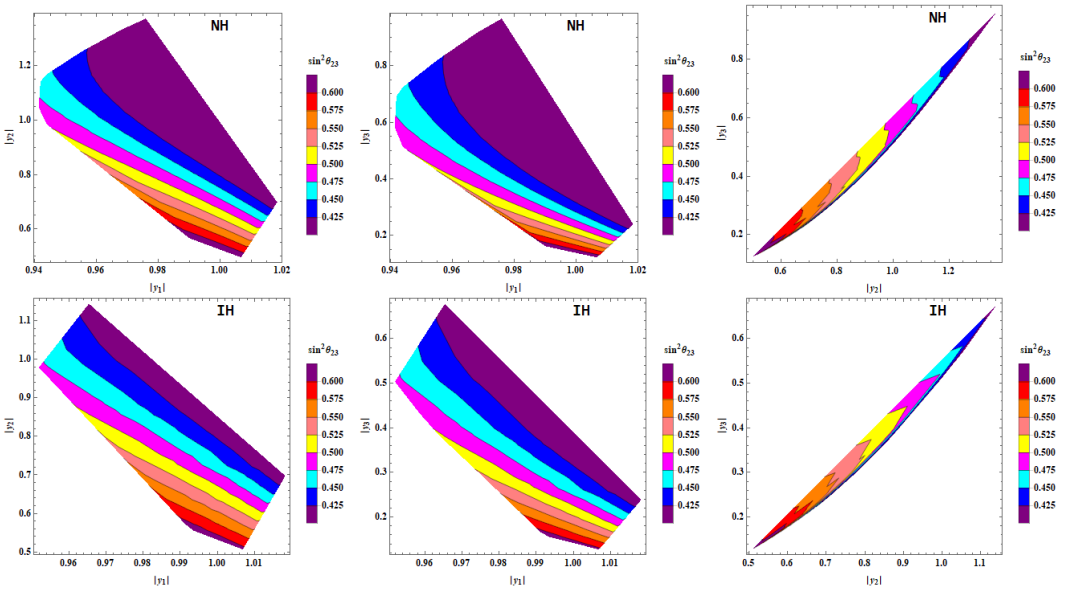

Figure 3.4: Contour plots of the Yukawa modular forms with the atmospheric mixing angle (θ_{23}).

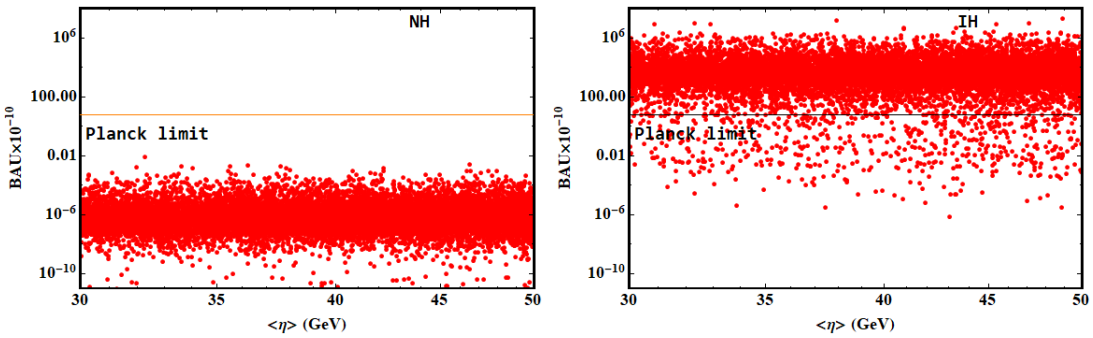

Figure 3.5: Variation between $<\eta>$ and Baryon asymmetry of the universe.

values of BAU which satisfy the Planck limit. This value of BAU for normal ordering is mainly concentrated in between (100-1000) GeV of M_1. Beyond this mass range the values of asymmetry is very less. But for inverted ordering this mass range is found to lie in between (100-5000) GeV. From this discussion it is clear that the values of baryon asymmetry of the universe can be obtained for both the hierarchies from this model.

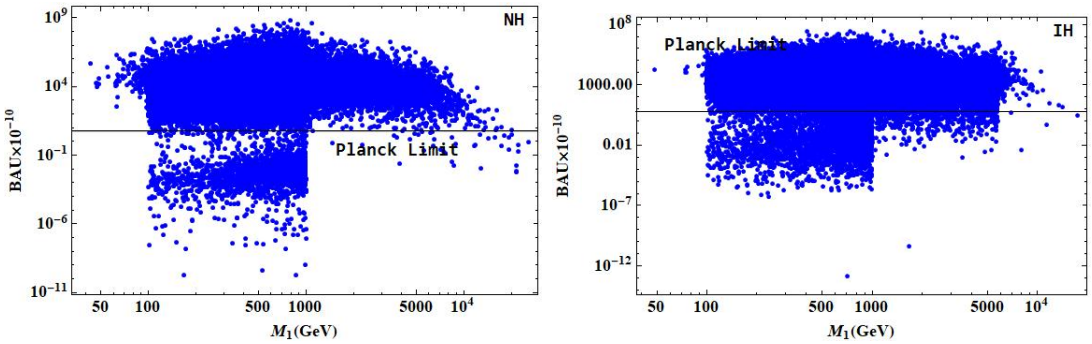

Figure 3.6: The figures above show the corelation between BAU and M_1 for both the hierarchies. In these figures, the horizontal lines represent the Planck value of BAU.

3.5.6 Relation of relic density of DM and $< \sigma v >$ with M_1

Now in Fig. (3.7) and (3.8) we show the variation of dark matter relic density and thermally averaged annihilation cross-section with respect to lightest heavy neutrino M_1. It can be seen that for M_1 in between (100-450) GeV, the values of relic density is more prominent for both the hierarchies. However, in case of inverted hierarchy, there are certain areas of mass that produce the observed relic density. As for the thermally averaged cross-section, we see that for almost the entire mass range of M_1, the values of the scattering cross section is consistent with the indirect detection limits [185].

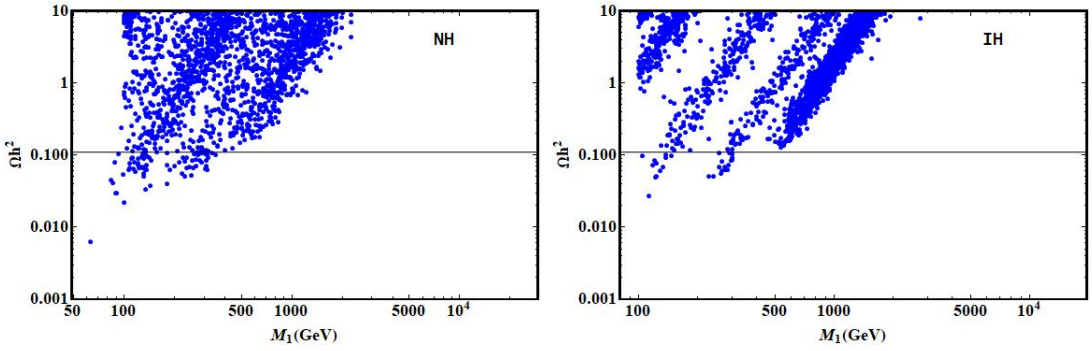

Figure 3.7: The above figure shows the variation between DM relic density and lightest right-handed neutrino M_1. The horizontal line represents the current dark matter abundance in the universe.

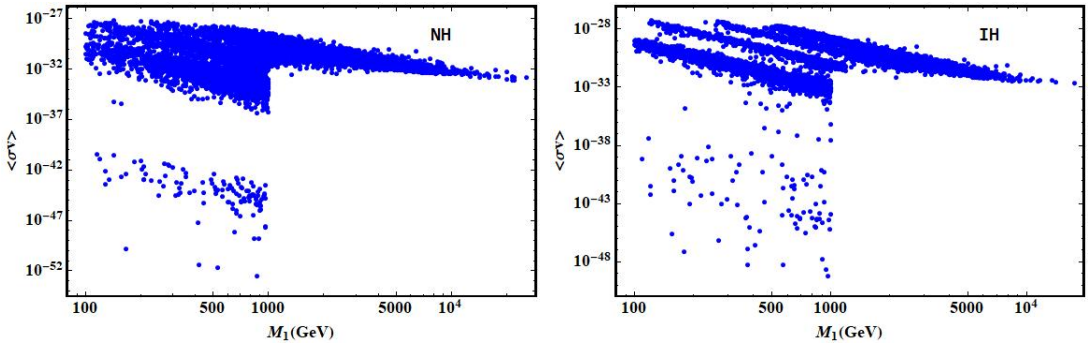

Figure 3.8: The above figure shows the corelation between cross-section $<\sigma v>$ and M_1.

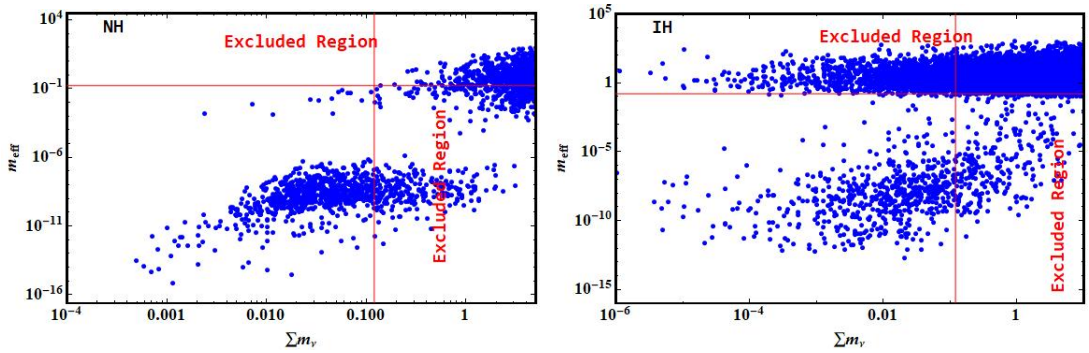

Figure 3.9: The figures above illustrate the corelation between $\sum m_\nu$ and m_{eff}. The vertical and horizontal lines represent their upper bounds.

3.5.7 Variation between m_{eff} and $\sum m_\nu$

We have also studied the effect of NDBD in this work. For this we have evaluated the Majorana effective mass (m_{eff}) of electron neutrino. In Fig. (3.9) we have shown the relation between sum of neutrino mass ($\sum m_\nu$) and effecive mass (m_{eff}) in our work. The recent cosmological findings provide the upper bound of $\sum m_\nu \leq 0.12$ eV, whereas the allowed range for the effective neutrino mass for NDBD as given by KamLAND-ZEN is found to be ≤ 0.165 eV. The horizontal line in the figure represents the upper bound of effective electron neutrino mass, whereas the vertical line represents the upper bound for sum of neutrino mass. It is quite evident from both the graphs that the model is able to generate sufficient parameter space within the allowed range for both the normal and inverted orderings.

3.6 Conclusion

In this chapter of the thesis we have presented our work on baryon asymmetry of the universe and dark matter. Accordingly we have extended the minimal inverse seesaw by adding an extra Higgs-type scalar triplet (η) to its particle content. We have used A_4 modular symmetry and Z_3 symmetry group in our work. On studying BAU in this model, we have obtained a satisfying parameter space corresponding to M_1 which abide by the Planck limit for both NO/IO. Again, we have extended our investigation to dark matter sector as well by calculating the relic abundance and annihilation cross section of the DM candidate. From plots in Fig. 3.7 and 3.8, we have obtained a certain region for M_1 mass which generates the observed relic abundance. Also, we have sufficient points which showcase very small scattering cross section. Thus, from the study of various phenomena that we have carried out in this work, we can have a conclusive idea that this model is a viable one.